Table 3 General-aviation aircraft hours flown

Year	Aircraft hours
1969	25,351,000
1970	26,030,000
1971	25,512,000
1972	26,974,000
1973	29,974,000
1974	31,413,000
1975	32,024,000
1976	33,922,000
1977	35,792,000
1978	36,600,000
Average	30,359,000

Table 4 Mid-air collision accidents, U.S. civil aviation (1969-1978)

Year	General aviation with general aviation	General aviation with air carrier	Air carrier with air carrier
1969	23	3	0
1970	32[b]	0	0
1971	27	3	0
1972	24[b]	1	0
1973	24	0	0
1974	32	0	0
1975	28	0	0
1976	30	0	0
1977	34	0	0
1978 (partial)[a]	33	1	0
Average	28.7	0.80	0

[a] 1978 files as of Sept. 26, 1978.
[b] Includes one U.S. general-aviation vs foreign aircraft.

Table 5 Comparison of random collision theory predictions with reported data (1969-1978)

Type of collision	Predicted rate collisions/yr	Actual rate collisions/yr	Factor by which human control influences rates
$\left(\frac{\text{General aviation}}{\text{General aviation}}\right)$	34.3	28.7	1.20
$\left(\frac{\text{General aviation}}{\text{Air carrier}}\right)$	590	0.80	738
$\left(\frac{\text{Air carrier}}{\text{Air carrier}}\right)$	99.4	0	∞

Comparing this number with the total number of registered general-aviation aircraft (Table 1) shows that at any given time on the average over the ten-year span 1.77% of the registered aircraft are in flight.

The final data of concern are the actual (recorded) number of mid-air collision accidents in U.S. civil aviation. These data of interest are presented in Table 4.[5] It is seen that the largest number of collisions occur between general-aviation aircraft.

The question arises as to what type of aircraft are characteristic of each of the two groups (general aviation and air carrier). To accurately determine these characteristics, a detailed analysis of the dimensions, speeds, and service ceilings of all aircraft is required. Lacking such input, the author has chosen the following aircraft as representative:

General aviation (small)—Cessna Model 150; 33-ft 2-in. wingspan; 23-ft 8-in. long; 9-ft 7-in. high; average cruising speed 117 mph; service ceiling 14,000 ft.

Air carrier (large)—Boeing Model 747; 195-ft 8-in. wingspan; 231-ft 10-in. long; 63-ft 5-in. high; average cruising speed 450 mph; service ceiling 39,000 ft.

While this exact choice may be disputed, the general features should be reasonably representative. The volume of the space is taken as the product of the service ceiling and the land area of the United States (3.60×10^6 miles^2).

Results and Discussion

Given the previous data, Eqs. (2) and (6) were used to predict the collision rate for comparison with the data of Table 4. A summary of the results is given in Table 5.

The comparisons between random collision theoretical predictions and the actual cases shown in Table 5 clearly show that insofar as mid-air collision accidents are concerned, human control is very effective in air-carrier travel, but relatively ineffective in general aviation. The reasons for this rather striking difference may possibly be in traffic control, pilot training, instrumentation, or whatever, but the analysis of such causes are not within the scope of this Note. Nevertheless, they should give cause for credit to air-carrier aviation and cause for concerns to general aviation.

Probably the weakest link in the previous analysis is the rather arbitrary choice of representative aircraft for the two groups considered. In this respect, a more detailed analysis is required for general-aviation aircraft. However, the comparisons for air carriers are relatively insensitive to the choice. For those trained in the physical sciences, the fact that random collision theory predictions are close to the "real world" for general aviation is, in itself, a remarkable revelation. It is the hope of this author that the information presented in this Note will have a positive influence on the marvelous, man-made world of aviation.

References

[1] Glasstone, S. and Sesonske, A., *Nuclear Reactor Engineering*, Van Nostrand Rheingold Co., New York, 1967, p. 71.

[2] Census of U.S. Civil Aircraft, 1971, U.S. Department of Transportation, FAA.

[3] Census of U.S. Civil Aircraft, calendar year 1978, U.S. Department of Transportation, FAA.

[4] "FAA Statistical Handbook of Aviation," U.S. Department of Transportation, FAA.

[5] "Mid-Air Collision Accidents, U.S. Civil Aviation, 1957-1978," National Transportation Safety Board, Washington, D.C.

AIAA 82-4005

Subsonic Flow over Airborne Optical Turrets

A. J. Laderman*
Ford Aerospace and Communications Corporation, Newport Beach, Calif.
and
R. de Jonckheere†
Air Force Weapons Laboratory, Kirtland Air Force Base, N. Mex.

Introduction

FOR a number of applications, the telescope of an airborne optical system is housed within a turret mounted atop the aircraft fuselage. The interaction of the turret with the high

Received June 1, 1981; revision received Sept. 14, 1981.

*Principal Scientist, Thermo-Fluid Dynamics Section. Member AIAA.
†Captain, USAF. Member AIAA.

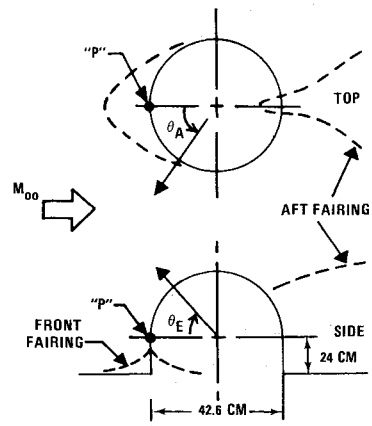

Fig. 1 Turret model.

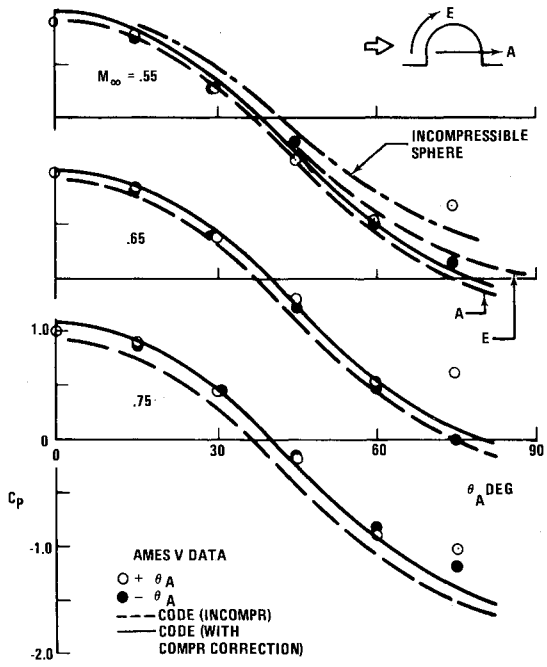

Fig. 2 Comparison of surface pressure measurements to compressibility corrected code.

subsonic airstream, however, can significantly influence the optical performance of the system. In recognition of this problem, considerable experimental effort has been devoted to determine the general nature of the turret flowfield.[1] While these studies have shown that flow separation occurs consistently on the aft portion of the turret, data concerning the attached flow over the forward surface is sparse. Although several test programs[2] have provided surface pressure measurements, a systematic assessment of this data is lacking and a commonly accepted model of pressure distribution does not yet exist. The lack of such information impacts the turret design. In particular, the effects of compressibility on the inviscid flow, which may be significant for the blunt turrets, have not been resolved. This problem is addressed here where we present a baseline relation for the pressure distribution in the attached flow region over a typical turret configuration and substantiate its validity by comparison with data. Details of the study are described in Ref. 3 while significant findings are reported here.

Turret Flowfield

The typical turret configuration, comprised of a hemisphere with a cylinder base, and including fore and aft fairings, is shown in Fig. 1, which includes also the turret dimensions. The turret is mounted on a flat plate oriented parallel to the freestream flow. (Replacing the flat plate with a cylinder to simulate the aircraft fuselage has little effect on the turret flowfield.) While the test model was provided with either an open or closed port telescope aperture, we direct our attention to the attached flow over the smooth uninterrupted turret surface. In particular, since separation occurs near the shoulder of the model, we confine this study to θ_A, $\theta_E < 90$ deg, where the latter are the azimuthal and elevation angles measured from the radius passing through point P, Fig. 1.

The inviscid flow over the turret was determined using the FACC Potential Flow Code, which utilizes the source-sink method developed by Hess and Smith.[4] The code applies only to attached flow and, therefore, is restricted to the forward half of the turret. While the code can be applied to blunt bodies typical of the turret, it is valid only for low speeds. Corrections for compressibility must be introduced once the incompressible flowfield has been determined. The results of the code calculations are expressed in terms of the pressure coefficient C_p, which has its usual definition

$$C_p = (\tfrac{1}{2})(P - P_\infty)/\rho_\infty U_\infty^2 \tag{1}$$

where P is the pressure, ρ is the density, U is the velocity, and subscript ∞ denotes the freestream value. A plot of the incompressible C_p distribution over the top of the turret, and along the surface ray corresponding to the hemisphere-cylinder junction, is shown in Fig. 2 which, for comparison, includes the results for a simple incompressible sphere model. Note that, in spite of the proximity of the cylindrical base, the predicted flow over the entire forward portion of the hemisphere cap is sphere-like in nature.

The AFWL has conducted a series of wind tunnel programs, designated the AMES Aero/Optic I-V tests, devoted to investigation of turret aerodynamics. The tests were performed in the NASA Ames 14-ft Transonic Wind Tunnel. The AMES III to V programs involved turrets of similar size and geometry and the surface pressure measurements from these tests were found to be in good agreement.[3] Consequently, we will use the AMES V measurements[3] as representative data for comparison with the code. These tests were conducted for freestream Mach number $M_\infty = 0.55$, 0.65, 0.75 with unit Reynolds number $\approx 10^7$ m^{-1}. Test results are shown in Fig. 2 where only data upstream of the aperture has been plotted so that the resulting C_p distribution corresponds to that for a smooth, uninterrupted turret (without aperture effects) extending from -90 deg $\leq \theta_A \leq +90$ deg, $\theta_E = 0$. We see that: 1) the compressible flow test data for C_p are in accord with the inviscid, incompressible code predictions and 2) there is a small, but consistent, compressibility effect that causes the observed C_p to increase slightly with increasing M_∞.

Compressibility Correction

A reliable method for estimating the observed compressibility effect was provided by the experimental data of Hsieh[5] who measured pressure distributions on a hemisphere model with a cylinder afterbody. In spite of the difference in model geometries, the present findings indicate that the flow over the turret is also sphere-like and, therefore, is similar to Hsieh's flowfield. In addition, the departure of the C_p distributions of Hsieh from the inviscid, incompressible sphere relation was similar in trend and magnitude to that observed between test and theory for the present turret model. Hsieh's data has been correlated by Grabow[6] in the form

$$C_p = A - B\sin^2\theta \tag{2}$$

where A and B are coefficients dependent on M_∞, and $A = 1.0$ and $B = 2.25$ for $M_\infty = 0$. A plot of the terms A and $B - A$ vs M_∞ is shown in Fig. 3 which included also a plot of the

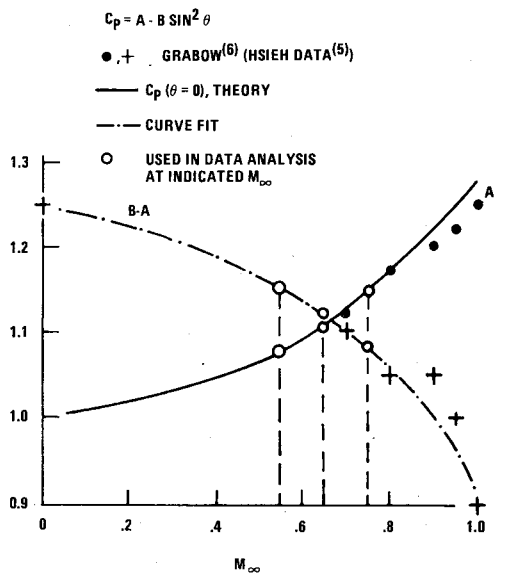

Fig. 3 Compressibility corrections to incompressible C_p distribution.

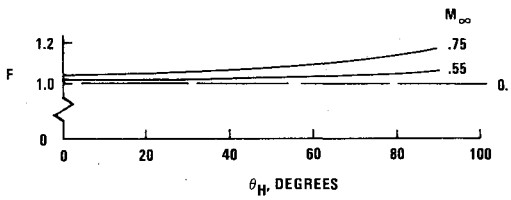

Fig. 4 Compressibility correction factor F.

theoretical stagnation point values from Eq. (1). The agreement between the latter and the coefficient A is quite good and substantiates both the data and the curve fit, Eq. (2). Figure 3 and Eq. (2) provide then the basis for the compressibility correlation described below.

The location of any point on the hemispherical portion of the turret can be defined by a single coordinate θ_T representing the included angle between the radius passing through the point and one passing through the point P (Fig. 1). Because of the asymmetry of the turret, C_p may not be identical for a given θ_T, (see rays A and E in Fig. 2) although the differences are small. We assume, however, that the angle θ_T has a single corresponding location θ_H on Hsieh's axisymmetric model. This implies that although C_p varies slightly for a given θ_T, the compressibility correction is the same and is defined by its value at θ_H. We define a correction factor F as

$$F_H(\theta_H, M_\infty) = \left(\frac{P/P_\infty(\theta_H, M_\infty)_c}{P/P_\infty(\theta_H)_i} \right)_{\text{Hsieh}} \tag{3}$$

where subscripts c and i denote the compressible and incompressible conditions, respectively. From the potential flow solution to the turret flowfield we find C_{p_i} and evaluate $P/P_\infty(\theta_T)_i$ from Eq. (1). Since we assume that $F_H(\theta_H, M_\infty) = F_T(\theta_T, M_\infty)$, the compressibility corrected pressure ratio is given then by

$$P/P_\infty(\theta_T, M_\infty)_c = F_H(\theta_H, M_\infty) P/P_\infty(\theta_T)_i \tag{4}$$

and finally, $C_{p_c}(\theta_T, M_\infty)$ is found from Eq. (1). The factor F has been plotted vs θ_T in Fig. 4 which shows that, for the indicated Mach number range, the effect of compressibility on P is small. The compressibility corrected C_p distribution is plotted in Fig. 2 where it is shown to have the proper trend and magnitude and to provide excellent agreement with the data.

Summary

It has been shown that a reasonable estimate of the turret C_p distribution in the region of attached flow is provided using an incompressible, inviscid code, which was successful in rationalizing the results of wind tunnel test measurements and which accounts for the effects of the turret configuration. In particular, for the M_∞ range considered here, compressibility effects were found to be small. However, an improved agreement between data and analysis is obtained using the code together with a compressibility correction proposed in this report.

Acknowledgment

This work supported by the USAF Weapons Laboratory, Kirtland AFB, under Contract F2960-79-C-0010.

References

[1] *Proceedings of the Aero-Optics Symposium on Electromagnetic Wave Propagation from Aircraft,* NASA Conference Publication 2121, April 1980.

[2] Steenken, W.G., "Wind Tunnel Investigation of 0.3-Scale APT Closed-Port Turret and Fairing Model," Convair Aerospace Division of General Dynamics, Report FZA-458-2, Jan. 1973.

[3] Laderman, A.J., "Surface Pressure Distribution Over an Airborne HEL Turret," Ford Aerospace and Communications, Newport Beach, Calif., FACC Report U-6680, March 1981.

[4] Hess, J.L. and Smith, A.M.O., "Calculation of Non-Lifting Body Potential Flow About Arbitrary Three Dimensional Bodies," McDonnell Douglas Report E.S. 40622, March 1962.

[5] Hsieh, T., "Hemisphere-Cylinder in Transonic Flow, $M_\infty = 0.7 \sim 1.0$," *AIAA Journal,* Vol. 13, Oct. 1975, pp. 1411-1413.

[6] Grabow, R.M., Ford Aerospace, private communication, 1981.

AIAA 82-4006

ADEN Plume Flow Properties for Infrared Analysis

Chong-Wei Chu* and Joe Der Jr.†
Northrop Corporation, Hawthorne, Calif.

IN Ref. 1 a simple modeling technique was presented to predict two-dimensional-nozzle plume properties for IR signature analysis. Models were developed and validated through comparisons with test data for two-dimensional converging-diverging (CD) and two-dimensional plug nozzles exhausting into quiescent air. The modeling technique was subsequently extended to an augmented deflecting exhaust nozzle (ADEN) with bypass ratios up to unity and with the engine swirl effectively accounted for in the model.[2] This Note presents the predicted plume properties for an ADEN [with a bypass ratio (BPR) of 0.25] with and without consideration of the engine swirl, and shows the striking effect of a 10-deg engine swirl‡ on the plume total temperature distributions. Such effects were first recognized in Ref. 3.

Figure 1 shows the predicted total temperature contours in the plume of an ADEN with a nozzle pressure ratio (NPR) of 2.76 and a zero bypass ratio and maximum exit total tem-

Received June 23, 1981.

*Senior Scientist, Department of Propulsion Research, Aircraft Division. Member AIAA.

†Senior Technical Specialist, Department of Propulsion Research, Aircraft Division. Associate Fellow AIAA.

‡The swirl angle is defined as the arc tangent of the ratio between the swirl and axial velocities.